First Direct Observation of Coulomb Explosion during the Formation of Exotic Atoms

T. Siems, D. F. Anagnostopoulos,* G. Borchert, and D. Gotta
Institut für Kernphysik, Forschungszentrum Jülich, D-52425 Jülich, Germany

P. Hauser, K. Kirch,† and L. M. Simons
Paul-Scherrer-Institut (PSI), CH 5232-Villigen, Switzerland

P. El-Khoury and P. Indelicato
Laboratoire Kastler-Brossel, UA 018 of the CNRS, Case 74, Université Pierre et Marie Curie, 4 place Jussieu, F-75252 Paris Cedex 05, France

M. Augsburger, D. Chatellard, and J.-P. Egger
Institut de Physique de l' Université de Neuchâtel, CH-2000 Neuchâtel, Switzerland
(Received 24 November 1999)

A Doppler broadening of x-ray transitions from pionic nitrogen and muonic oxygen, which is attributed to Coulomb explosion of the molecules, has been observed by using a crystal spectrometer. Large linewidths indicate fast ionization of the molecules and a charge of $(3-4)e$ for the accelerated fragments.

PACS numbers: 36.10.–k, 07.85.–m, 32.30.Rj

In molecules, the emission of binding electrons is ultimately accompanied by an energetic fragmentation of the atoms, a phenomenon referred to as Coulomb explosion. The fragmentation is usually achieved by intense laser fields [1,2], heavy-ion bombardment [3,4], stripping in thin foils [5], or soft x rays [6].

Evidence for Coulomb explosion following the capture of heavy negatively charged particles was obtained from experiments with muonic atoms [7]. From a comparison of Lyman transitions of diatomic targets such as nitrogen with monoatomic gases such as neon at various gas pressures, it was found, that the Lyman yields in muonic nitrogen were similar to those in neon, but at much lower pressures [8]. The difference was interpreted to originate from the higher velocity of the muonic nitrogen system caused by Coulomb explosion, which results in an enhanced electron refilling. The refilling rate is given by $W_{\mathrm{ref}} = N v \sigma_{\mathrm{ref}}$, with N being the density of the target material and v the velocity of the exotic atom relative to the surrounding atoms [9]. The cross section σ_{ref} depends, in general, on the charge state and the velocity. The gross approximations made in [8], as independence of σ_{ref} on v and similarity of refilling and of cascades in nitrogen and neon, did not allow a quantitative extraction of the charge state and v at the instant of the Coulomb explosion from the Lyman yields.

The formation and the first steps of the deexcitation of an exotic atom proceed via Auger emission, excitation, and self-ionization first of the molecular [10] and, subsequently, of the atomic electron shell, which quickly leads to a high degree of ionization. In the case of muons and for noble gases with atomic numbers $Z \leq 18$, almost complete ionization has been demonstrated for pressures below 0.2 bar [11,12] showing that electron refilling from surrounding atoms or molecules can be excluded under such conditions. Moreover, the kinetic energy of the exotic atom immediately after formation is assumed to be in the region of several eV [13].

The results presented here were obtained from a study of linewidths of pionic and muonic x rays in the preparation of an experiment at the Paul-Scherrer-Institut (PSI) aiming at an improved determination of the charged pion mass [14–16]. The pion mass will be determined from the πN$(5g\text{-}4f)$ transition using the same transition in μO as calibration standard for a reflection-type crystal spectrometer (setup in Johann geometry [17,18]). The resolution function will be obtained from the $\pi\,^{20}$Ne$(6h\text{-}5g)$ transition (Table I).

The experimental setup was similar to the one described in [15]. Using the 105 MeV/c pion beam in the $\pi E5$ area at PSI, about $4 \times 10^8\ \pi^-$/s were injected into the new cyclotron trap [20] at a proton current of 1 mA from the accelerator. A gas-filled cylindrical container of 230 mm length, a diameter of 60 mm, and of 50 μm thick Kapton walls was used as target. About $10^6\ \pi^-$/s were stopped in the gas at a pressure of 1 bar. Some of the pions

TABLE I. X-ray energies E_{X} as calculated for an exotic atom without any remaining electrons, and crystal parameters Bragg angle Θ_{B}, intrinsic resolution ω_f, and dispersion $dE/d\Theta$ for the Si(220) reflection. The natural linewidths of the x-ray transitions are of the order of 10 meV, which is negligibly small compared to the experimental resolution. Θ_{B}, which includes the index of refraction shift, and ω_f were calculated by using the code XDF [19] for plane crystals.

Transition	E_{X} (eV)	Θ_B	ω_f ($''$)	$dE/d\Theta$ (meV/$''$)
$\pi\,^{20}$Ne$(6h\text{-}5g)$	4509.888	45°43′2.6″	12.5	21.32
$\pi\,^{14}N(5g\text{-}4f)$	4055.373	52°45′47.2″	14.5	14.94
$\mu\,^{16}$O$(5g_{7/2}\text{-}4f_{5/2})$	4024.308	53°20′43.2″	14.7	14.51
$\mu\,^{16}$O$(5g_{9/2}\text{-}4f_{7/2})$	4023.757	53°21′21.2″	14.7	14.51

decelerating inside the cyclotron trap decayed into muons. Of these, 10^5 μ^-/s were stopped in the gas.

The spectrometer was equipped with spherically bent silicon 110 crystals of 100 mm diameter and a radius of curvature of $R_c = 2985.4$ mm. In order to avoid edge effects from bending, the crystals were covered with a diaphragm of 95 mm free diameter (∅95). A two-dimensional picture of the reflected x rays was recorded with charge-coupled devices (CCDs) allowing to correct for the curvature of the image before being projected to the axis of dispersion. With the small pixel size of 22.5 μm and good energy resolution of about 200 eV FWHM (at 4 keV) of the CCDs, an efficient background reduction was achieved by the analysis of the hit pattern. Charged particles, x rays of higher energies, and γ rays deposit energy in several neighboring pixels and can therefore be discriminated against low-energy x ray events, which deposit charge only in one or two adjacent pixels. About 100 events per hour were detected in the pionic lines (Fig. 1). The rate for muonic x rays was a factor of 20 less because of the more extended muon stop distribution.

Three crystals denoted $Z15$, $Z30$, and $Z31$ [21] were used in this experiment. In all cases, the linewidths found for the πN and μO transitions were significantly larger than in the case of πNe (Table II). In an earlier high-statistics measurement of the πN transition using also the crystal $Z15$ [15], a FWHM of almost 50″ (seconds of arc) was found corroborating the present findings.

In the Johann geometry, the crystal surface does not follow the Rowland circle. This causes an aberration effect in the direction of dispersion (Johann broadening) proportional to $(\cot\Theta_B \cdot b_c/R_c)^2$, where b_c denotes the horizontal extension of the crystal. Simulating the experiment with a Monte Carlo ray-tracing code, which includes the geometrical broadening, for the diaphragm ∅95 mm a linewidth of 22″ (FWHM) was obtained for the πN$e(6h\text{-}5g)$ transition. This value is the theoretical limit in resolution for that geometry. When reducing the reflecting area horizontally to 60 mm (see below), the limit for the linewidth decreases to 15″.

The measured line shape of the $\pi\,^{20}$Ne$(6h\text{-}5g)$ transition yielded sizable contributions to the linewidth, which cannot originate from the intrinsic crystal resolution or geometrical aberrations. Studies of the imaging properties of the crystal $Z31$ by means of optical methods showed surface distortions, which were attributed to an imperfect bending of the silicon plates into a sphere. The deviations from a perfect surface were found to be up to 10″, which is sufficient to explain the broadening observed for $Z30$ and $Z31$. The difference between $Z31$ and $Z15$ is due to distortions of the silicon bulk material [15]. The crystals $Z30$ and $Z31$ are assumed to be identical because they were manufactured in the same process from the same silicon bulk material of superior quality. No differences were found from studies using Sc$K\alpha$ x rays.

To study the effects of the Johann broadening, a second diaphragm was attached to the crystals $Z30$ and $Z31$, which limited the horizontal extension to 60 mm (||60). For πN, the linewidth did not change within the errors when crystal or diaphragm were changed (Table II). In the case of πNe, distinct differences showed up for the two diaphragms, which are attributed to the Johann broadening (Fig. 2). From a Monte Carlo ray-tracing calculation at the wavelength of the πN transition, now including an additional broadening owing to the crystal distortion, for the linewidth of the crystal $Z30$ values of 24″ and 18″ were found for the two diaphragms ∅95 mm and ||60 mm, respectively. In the range of Bragg angles between 45° and 53° (Table I), the widths of the reflections are constant within 1″for a given diaphragm as confirmed by the Monte Carlo simulation.

Hence, the linewidths of the πN and μO transitions are dominated by a broadening originating from effects related to the systems formed with the molecules N_2 and O_2. This additional width is interpreted as a Doppler broadening stemming from Coulomb explosion.

To quantify the Doppler contribution, the line shape was modeled by the convolution of the resolution function and rectangular boxes each corresponding to one specific charge state. The best approximation is achieved

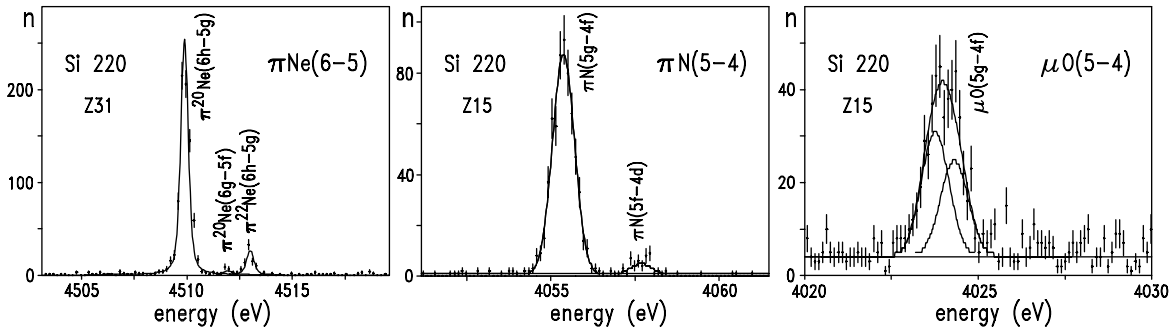

FIG. 1. Spectra of πNe$(6h\text{-}5g)$, πN(5-4), and μO(5-4) transitions measured at a gas pressure of 1 bar using a crystal diaphragm of ∅95 mm. In the πN and πNe spectra, the first parallel transitions $5f\text{-}4d$ and $6g\text{-}5f$ are visible. The relative intensity of the $\pi\,^{22}$Ne$(6h\text{-}5g)$ transition corresponds to the natural abundancy of the ^{22}Ne isotope. The μO line was fitted as a fine structure doublet. One channel corresponds to four CCD pixels of 22.5 μm.

TABLE II. Linewidths (FWHM) as measured with the three Si crystals labeled $Z15$, $Z30$, and $Z31$. The errors given are statistical only. A circular diaphragm covering the edge zones of the crystals is indicated by $\varnothing 95$ and an additional horizontal restriction by $||60$.

Transition	p (bar)	$Z15$ $\varnothing 95$ ($''$)	$Z30$ $\varnothing 95$ ($''$)	$Z30$ $\|\|60$ ($''$)	$Z31$ $\varnothing 95$ ($''$)	$Z31$ $\|\|60$ ($''$)
πNe($6h$-$5g$)	1.0	29.3 ± 1.2			25.7 ± 0.8	18.9 ± 0.9
πN($5g$-$4f$)	0.6	47.7 ± 1.3				
	1.0	51.5 ± 1.1	49.8 ± 1.7	48.3 ± 1.3	47.8 ± 1.7	
	2.5	54.8 ± 0.7				
μO($5g$-$4f$)	1.0	51.3 ± 6.8				

with one single box only. To search for a superposition of several charge states, the line shape was modeled by continuous functions, e.g., a Gaussian, which in all cases led to a significant increase of χ^2. The Doppler widths ΔE_C for the approach with one box are given in Table III. Applying this line-shape model to the resolution function from πNe yields the asymmetric contribution to the systematic error.

From the Doppler width, the potential energy $q_1 q_2 / r_{12}$ is deduced where q_1 and q_2 are the charges of the recoiling πN (μO) atom and the nitrogen (oxygen) ion and r_{12} is their distance at the instant of fragmentation. The values for $q_1 q_2$ as obtained from inserting the molecular bond length $r_{N_2} = 1.098$ Å ($r_{O_2} = 1.208$ Å) [22] are given in Table III.

The assumption of fragmentation at approximately the molecular bond length is supported by the time scale for the depletion of the electron shells. Auger emission is by far the fastest process in the upper and medium part of the atomic cascade. Typical Auger rates for atoms are at least 10^{16} s^{-1} for L electrons when the pion's (muon's) main quantum number n is about 25. Radiative decay rates are several orders of magnitude smaller [23,24]. The Auger rates in the "molecular" system πN_2 (μO_2) are assumed to be of the same order of magnitude as in the "atom." Shake-off effects may further speed up the ionization. Therefore, the pion (muon) is able to remove several if not all binding electrons in less than 1 fs.

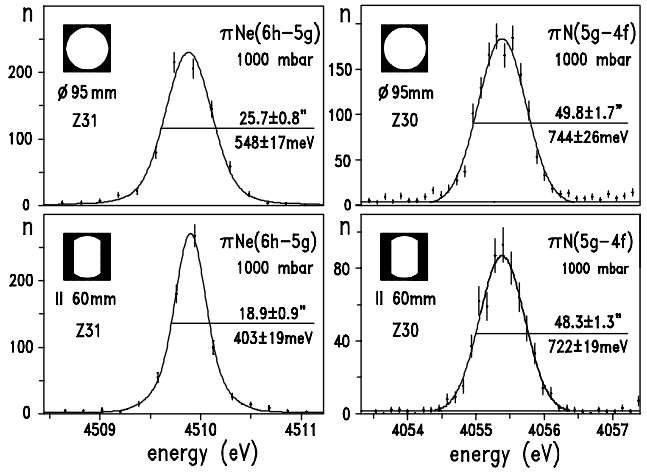

FIG. 2. π^{20}Ne($6h$-$5g$) and $\pi^{14}N$($5g$-$4f$) transitions measured with two different diaphragms (see Table II).

In laser-induced Coulomb explosion, fragmentation at distances up to 5 Å has been observed [1,2]. However, to reach that distance, it takes the two ions about 7 fs, which is longer than the time needed to deplete the electronic L shell in both atoms even if the pion or muon is already attached to one of the fragments. For fragmentation distances significantly larger than the molecular bond length, the two fragments must be ionized completely to explain the observed Doppler width. This, however, requires the very unlikely emission of K electrons from both ions.

The processes possible after separation of the molecule and before emission of the x ray are collision, refilling, radiative deexcitation, and K- and L-Auger emission. At a gas pressure of 1 bar, the average time between two collisions is 10^4 fs for a thermalized πN system, but only about 100 fs for velocities corresponding to the measured Doppler broadening. The radiative lifetime of the $5g$ state is 500 fs, whereas K-Auger emission takes place already after a few fs.

The cross sections both for collision and refilling are of the order of several 10^{-15} cm^2 [9]. Therefore, at gas pressures around 1 bar only a few collisions can happen before the emission of the ($5g$-$4f$) x ray with a mean energy loss per collision, which is small compared to the maximum possible energy transfer. Hence, the velocity derived from the Doppler broadening should be close to the one originating from the explosion of the molecule.

At the occurrence of the ($5g$-$4f$) transition, the electron shell of a πN (μO) system is completely depleted for the target densities considered here. Otherwise, because of the short Auger lifetime, x radiation would be strongly suppressed [11]. The observation of circular transitions with high yields from levels up to $n = 7$ proves that for the transitions measured in this experiment the cascade develops mostly through the high angular-momentum states [12]. At least the last two steps before populating the $5g$ or $6h$ states proceed mainly due to radiative deexcitation.

For a fragmentation distance of about the molecular bond length, the possible range of one fragment's charge

TABLE III. Coulomb explosion parameters. The symmetric error is statistical only. The systematic error is due to the various assumptions on the fitting procedure and the parametrization of the response function as derived from πNe. Polarization corrections [8] have not been considered.

	Crystal	p (mbar)	ΔE_C (meV)	v/c (10^{-6})	$q_1 q_2/r$ (eV)	$q_1 q_2/e^2$
πN($5g$-$4f$)	$Z15$ ∅95	620	$773 \pm 24^{+30}_{-74}$	$95 \pm 3^{+3}_{-8}$	$119 \pm 8^{+8}_{-22}$	$9.2 \pm 0.6^{+0.7}_{-1.7}$
		1000	$765 \pm 47^{+34}_{-78}$	$94 \pm 6^{+4}_{-9}$	$117 \pm 14^{+11}_{-24}$	$9.0 \pm 1.1^{+0.8}_{-1.8}$
		2500	$951 \pm 23^{+18}_{-62}$	$117 \pm 3^{+2}_{-7}$	$182 \pm 8^{+8}_{-24}$	$13.9 \pm 0.7^{+0.5}_{-1.8}$
	$Z30$ ∅95	1000	$805 \pm 30^{+15}_{-117}$	$99 \pm 3^{+2}_{-14}$	$130 \pm 11^{+6}_{-35}$	$10.0 \pm 0.8^{+0.4}_{-2.8}$
	$Z30$ ||60	1000	$855 \pm 26^{+52}_{-122}$	$105 \pm 3^{+6}_{-14}$	$146 \pm 8^{+16}_{-41}$	$11.2 \pm 0.6^{+1.2}_{-1.7}$
	$Z31$ ∅95	1050	$789 \pm 30^{+25}_{-127}$	$97 \pm 3^{+3}_{-15}$	$125 \pm 8^{+8}_{-38}$	$9.6 \pm 0.7^{+0.6}_{-2.9}$
μO($5g$-$4f$)	$Z15$ ∅95	1050	$992 \pm 98^{+233}_{-277}$	$123 \pm 12^{+29}_{-34}$	$230 \pm 45^{+95}_{-115}$	$19 \pm 4^{+9}_{-11}$

is between $2e$ and $6e$ (Table III). A symmetric configuration, i.e., $q_1 q_2/e^2 \sim 3 \times 3$ to $\sim 3 \times 4$, may originate from the complete removal of up to six binding electrons from the N_2 molecule with a subsequent fast emission of the remaining $2s$ electrons from the atom to which the pion is finally attached. A second possibility, resulting in asymmetric charge states, is separation after removal of 4 binding electrons leaving a N^{2+} and a $(\pi N)^{2+}$ system. The $(\pi N)^{2+}$ system, however, must then be ionized completely before the distance increases significantly.

An evidence for a pressure dependence was found from the πN($5g$-$4f$) transition (Tables II and III), which may be explained along the lines of the density effect observed in the line yields [8,12]. As the cascade proceeds at higher pressures in average through lower angular-momentum states, larger energy gains are possible for one deexcitation step. This in turn permits the emission of stronger bound electrons before separation. However, a detailed investigation based on up-to-date cascade models is necessary to prove the validity of such arguments.

In summary, the Doppler broadening of x-ray transitions originating from pion- and muon-induced Coulomb explosion has been observed directly for N_2 and O_2. Because of the symmetry of diatomic molecules acceleration is expected to be maximal. The charges of the recoiling fragments of $(3-4)e$ indicate a fast depletion of the molecular electron shell by Auger emission.

We would like to thank our technicians B. Leoni and K.-P. Wieder for their excellent work during the preparation of the experiment and the Carl Zeiss company for the very co-operative help setting up the Bragg crystals. We are grateful to F. Nez and L. Massou (Laboratoire Kastler-Brossel) and J. Jacubowiez and T. Avignon (Ecole Supérieure d'Optique) at the University P. et M. Curie for the optical crystal test. A NATO grant (Contract No. CRG960623) is acknowledged as well. D. F. A. is indebted to the European Union for its support (Contract No. FMBICT950378).

*Present address: Department of Materials Science and Engineering, University of Ioannina, Greece.
†Present address: Los Alamos National Laboratory, Los Alamos, NM 87545.

[1] J. H. Posthumus *et al.,* J. Phys. B, At. Mol. Opt. Phys. **29,** L525 (1996).
[2] C. Cornaggia *et al.,* Phys. Rev. A **44,** 4499 (1991).
[3] R. Mann *et al.,* Phys. Rev. Lett. **37,** 1674 (1976).
[4] Hai-Ping Cheng and J. D. Gillaspy, Phys. Rev. B **55,** 2628 (1997).
[5] M. P. Carpenter *et al.,* Phys. Rev. A **55,** 2090 (1997).
[6] W. Eberhardt *et al.,* Phys. Rev. Lett. **58,** 207 (1987).
[7] J. D. Knight *et al.,* Phys. Rev. A **27,** 2936 (1983).
[8] P. Ehrhardt *et al.,* Z. Phys. A **311,** 259 (1983).
[9] B. H. Bransden and M. R. C. McDowell, *Charge Exchange and Theory of Ion-Atom Collisions* (Clarendon Press, Oxford, 1992).
[10] L. I. Ponomarev, Annu. Rev. Nucl. Sci. **23,** 395 (1973).
[11] R. Bacher *et al.,* Phys. Rev. A **39,** 1610 (1989).
[12] K. Kirch *et al.,* Phys. Rev. A **59,** 3375 (1999).
[13] T. v. Egidy *et al.,* Phys. Rev. A **29,** 455 (1984).
[14] D. Anagnostopoulos *et al.,* PSI proposal R-97-02.1.
[15] S. Lenz *et al.,* Phys. Lett. B **416,** 50 (1998).
[16] T. Siems, Ph.D. thesis, University of Cologne, 1998 (unpublished).
[17] H. H. Johann, Z. Phys. **69,** 185 (1931).
[18] M. A. Blokhin, in *Advances in X-ray Spectroscopy,* edited by C. Bonnelle and C. Mandé (Pergamon Press, Oxford, 1982), pp. 90–103.
[19] Code XDF, in S. Brennan and P. L. Cowan, Rev. Sci. Instrum. **63,** 850 (1992).
[20] L. M. Simons, Phys. Scr. **T22,** 90 (1988); P. Hauser *et al.,* PSI-F1 newsletter1996, 1997, p. 11.
[21] The Bragg crystals were manufactured in collaboration with the Carl Zeiss company, Oberkochen, Germany.
[22] *Handbook of Chemistry and Physics* (CRC Press, Cleveland, Ohio, 1971), 52nd ed., p. F-174.
[23] G. R. Burbidge and A. H. de Borde, Phys. Rev. **89,** 189 (1953).
[24] F. J. Hartmann, in *Electromagnetic Cascade and Chemistry of Exotic Atoms,* edited by L. M. Simons, D. Horvàth, and G. Torelli (Plenum Press, New York, 1990), and references therein.